**Supporting Information for**

# Confined formation of ultrathin ZnO nanorods/reduced graphene oxide mesoporous nanocomposites for high-performance room-temperature $NO_2$ sensors

Yi Xia[a, b, #], Jing Wang[a, c, #, *], Jianlong Xu[d], Xian Li[e], Dan Xie[e], Lan Xiang[a, *], Sridhar Komarneni[c, *]

[a] Department of Chemical Engineering, Tsinghua University, Beijing, 100084, China

[b] Research Center for Analysis and Measurement, Kunming University of Science and Technology, Kunming 650093, China

[c] Department of Ecosystem Science and Management and Materials Research Institute, Materials Research Laboratory, The Pennsylvania State University, University Park, PA 16802, USA

[d] Institute of Functional Nano and Soft Materials (FUNSOM), Jiangsu Key Laboratory for Carbon-based Functional Materials and Devices, Soochow University, Suzhou, Jiangsu 215123, China

[e] Institute of Microelectronics, Tsinghua University, Beijing, 100084, China

# These two authors contributed equally.

*Corresponding authors. Email: wangjingflotu@gmail.com (J. Wang); xianglan@mail.tsinghua.edu.cn (L. Xiang); sxk7@psu.edu (S. Komarneni);

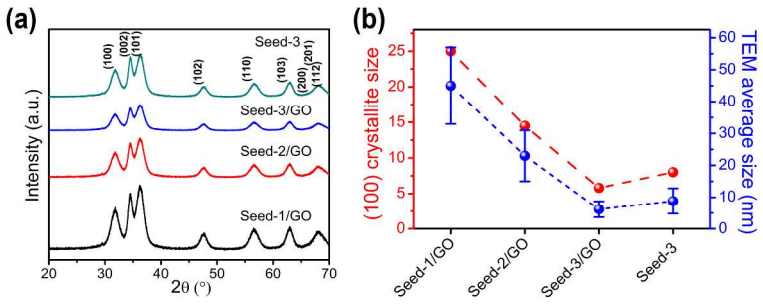


**Figure S1.** (a) XRD patterns of different nanoseeds; (b) summarized results of the calculated crystallite sizes from (100) diffraction peaks and the TEM observed average seed diameters.

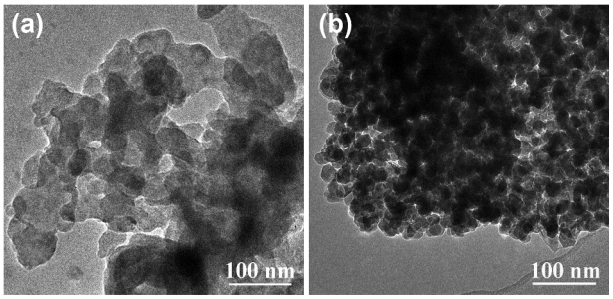


**Figure S2.** TEM images of the seed-1 (a) and seed-2 (b) formed in the absence of GO.

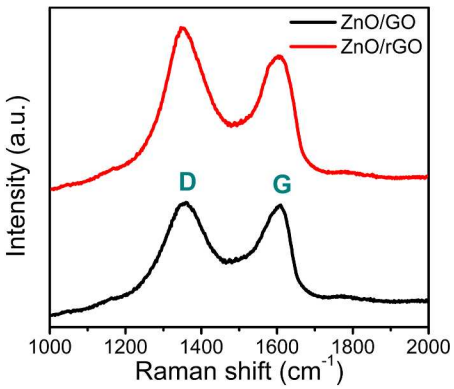


**Figure S3.** Raman spectra of ZnO nanoseeds/GO and ZnO nanorods/rGO.

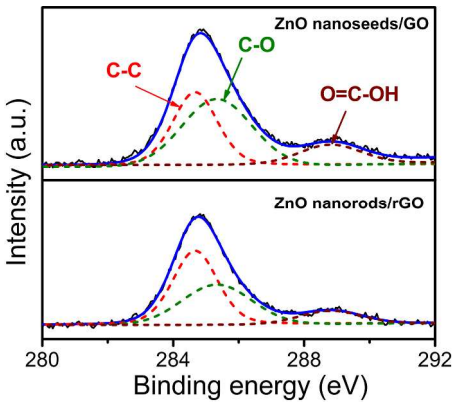


**Figure S4.** C 1s XPS spectra of ZnO nanoseeds/GO and ZnO nanorods/rGO.

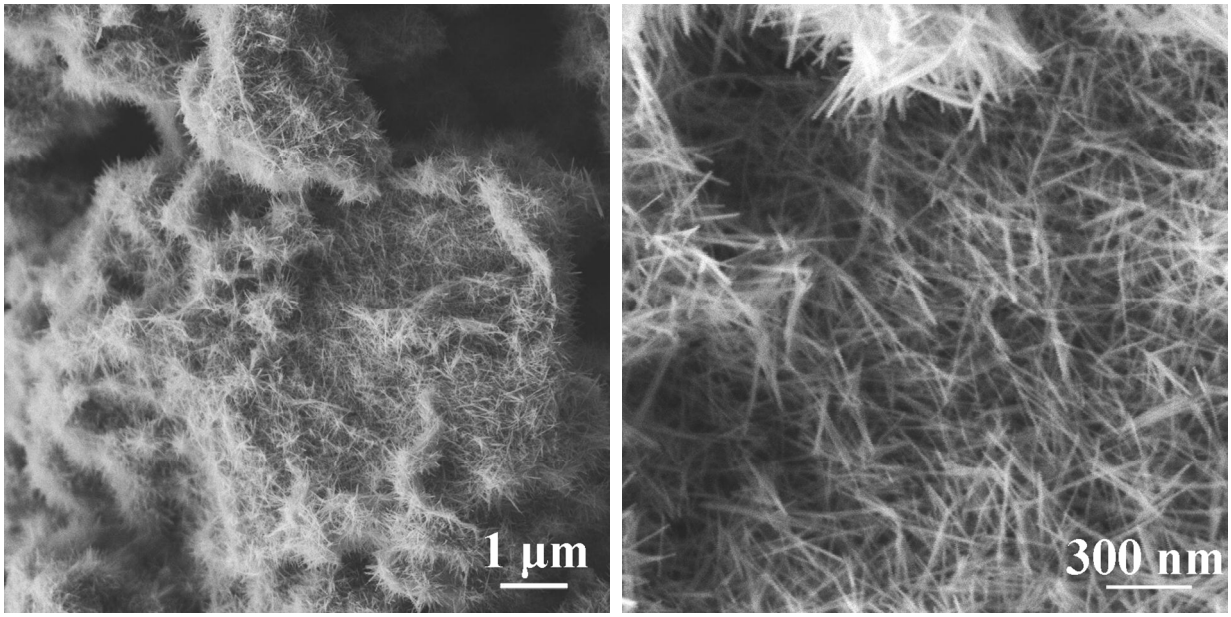


**Figure S5.** Enlarged Figure 2c and its inset.

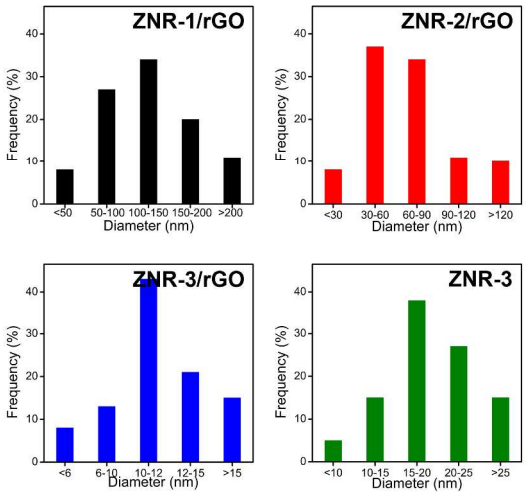


**Figure S6.** Diameter distributions of the nanorods in ZNR-1/rGO, ZNR-2/rGO, ZNR-3/rGO and ZNR-3.

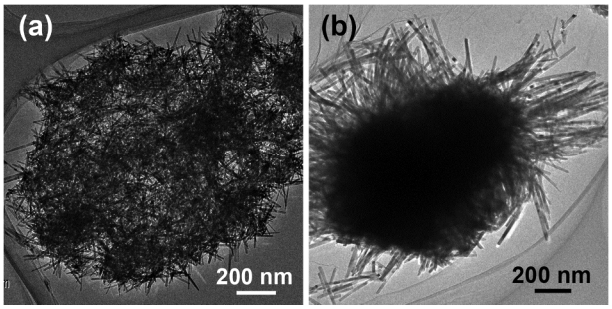


**Figure S7.** Low-magnitude TEM images of ZNR-3/rGO (a) and ZNR-3 (b).

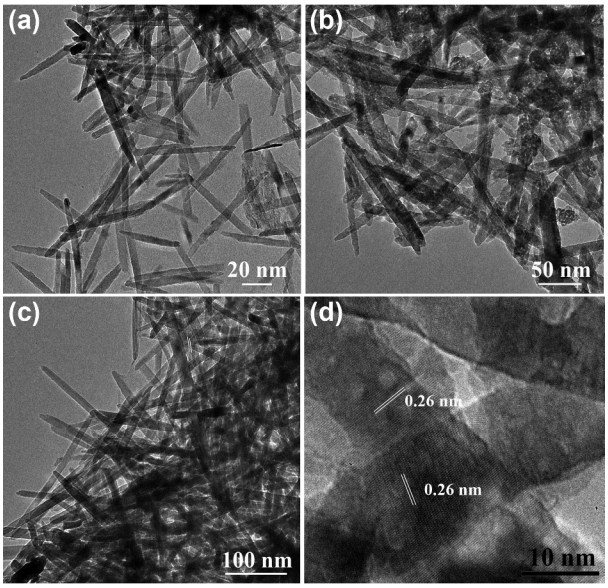


**Figure S8.** TEM and HRTEM images of ZNR-3/rGO at different reaction time (min). (a) 2; (b, d) 5 and (c) 10.

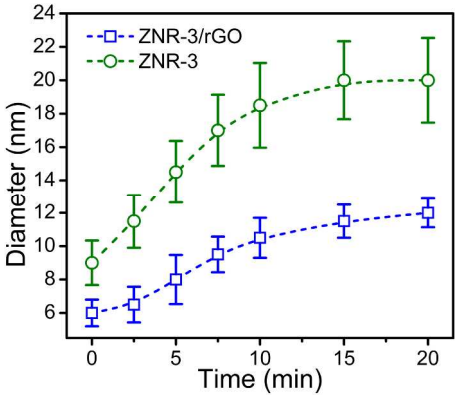


**Figure S9.** Variation of nanorod diameters during the growth of ZNR-3/rGO and ZNR-3.

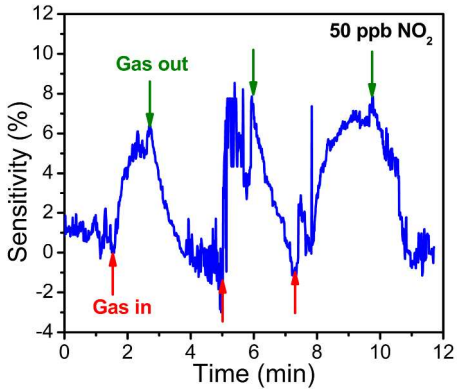


**Figure S10.** Dynamic response curve of the ZNR-3/rGO sensor to 50 ppb $NO_2$ for 3 cycles at 25 $^{o}$C.

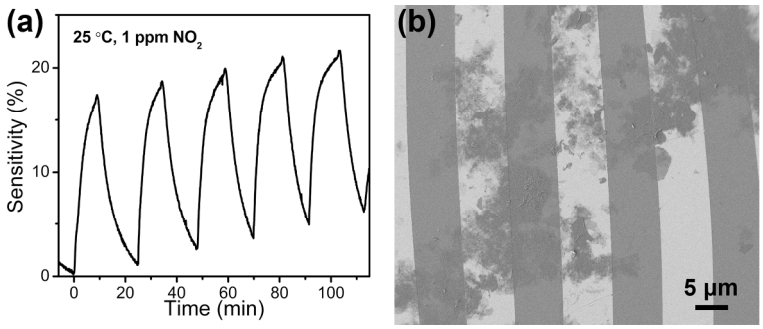


**Figure S11.** (a) Reproducibility of the rGO sensor to 1 ppm of $NO_2$; (b) SEM image of the rGO sensor.

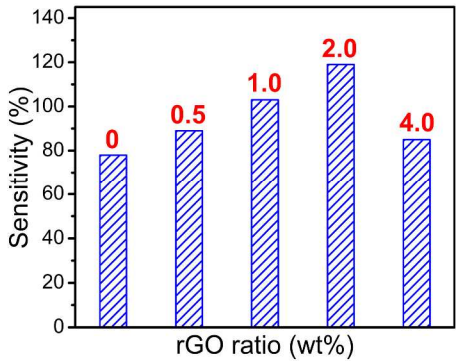


**Figure S12.** Effect of rGO ratio on the sensitivity of ZNR-3/rGO nanocomposites.

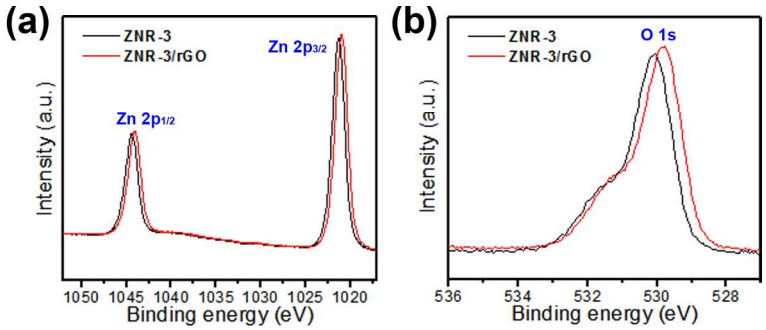


**Figure S13.** Zn 2p (a) and O 1s (b) XPS spectra of ZNR-3 and ZNR-3/rGO samples.